Characterizing Metabolic Inhibition Using Electrochemical Enzyme-DNA Biosensors

Supplemental Information

Additional Experimental Information.

Film Assembly PG Electrodes. Layer-by-layer films were assembled on basal plane pyrolytic graphite (PG, 0.16cm^2) disk electrodes machined from a PG block (Advanced Ceramics). Prior to film assembly, the PG electrodes were polished on 400 grit SiC paper (3M Crystal Bay), sonicated in pure water for 20-30s and dried with a stream of $N_{2\,(g)}$. An initial layer of PDDA is adsorbed for 15 minutes followed by rinsing in pure water. Successive layers of DNA (15mins), CYP101 (25mins) and PDDA were alternatively added to form the layer by layer. These conditions were previously optimized.[1] The film was assembled in the following manner $(PDDA/DNA/CYP101/)_2$-PDDA/DNA. The solution used for adsorption were as follows: 2mg mL^{-1} PDDA in 50 mM NaCl, 2mg mL^{-1} st-DNA in 10mM Tris pH 7.1/ 0.5M NaCl, and 1mg mL^{-1} CYP101 in 50 mM MES pH 5.6.

Quartz crystal microbalance (QCM, USI Japan, with a BK Precision frequency counter, Dynascan Corp) was used to monitor the film formation with a 9MHz QCM resonators (AT-cut, International Crystal Mfg.). To approximate the PG electrode surface of the polished PG electrode, a self-assembled monolayer of 3-mercaptopropionic acid (5 mM, in ethanol) made on the gold-coated (0.16 cm^2) QCM resonator for 1 hour. The SAM modified resonators were alternately washed with ethanol and pure water followed by drying with $N_{2\,(g)}$. The LBL films were then assembled as previously discussed with frequency measurements made before and after each layer. The adsorbed mass was measured using the Sauerbrey equation (1). Using a 9 MHz resonator the dry film mass per unit area (M/A) is described as:[1]

$$M / A(g / cm^2) = -\Delta F(Hz)(1.83 \times 10^8) \qquad (1)$$

The nominal thickness (d) of the dry film was estimated by an expression verified by high-resolution electron microscopy:[1]

$$d(nm) \approx (-0.016 \pm 0.002)\Delta F(Hz) \qquad (2)$$

Voltammetry. CH Instruments 1232, 660A and 430 potentiostats were used to conduct square wave voltammetry (SWV). A three electrode consisting of saturated calomel reference, platinum counter and film-coated PG was used to collect voltammograms. The square wave voltammograms were collect with a 4 mV step height, 25 mV pulse height and 10 Hz frequency. The supporting electrolyte consist of 50 mM NaH_2PO_4 pH 7.0/50mM NaCl with 50µM $Ru(bpy)_3Cl_2$ as the mediator.

Additional Results

Film Assembly. A (PDDA/DNA/CYP101/)$_2$PDDA-DNA layer-by-layer film was used to investigate the inhibition of DNA damage. Verification of reproducible film assembly was conducted using the decrease in QCM frequency as a function of successive layer deposition. The quartz resonator employed in QCM measurements was modified with a carboxyl terminated self-assembled monolayer to approximate the PG electrode surface. The QCM frequency decreased with successive layer deposition commensurate with film growth on the resonator (Figure 1). The growth was reproducible and pseudo-linear.

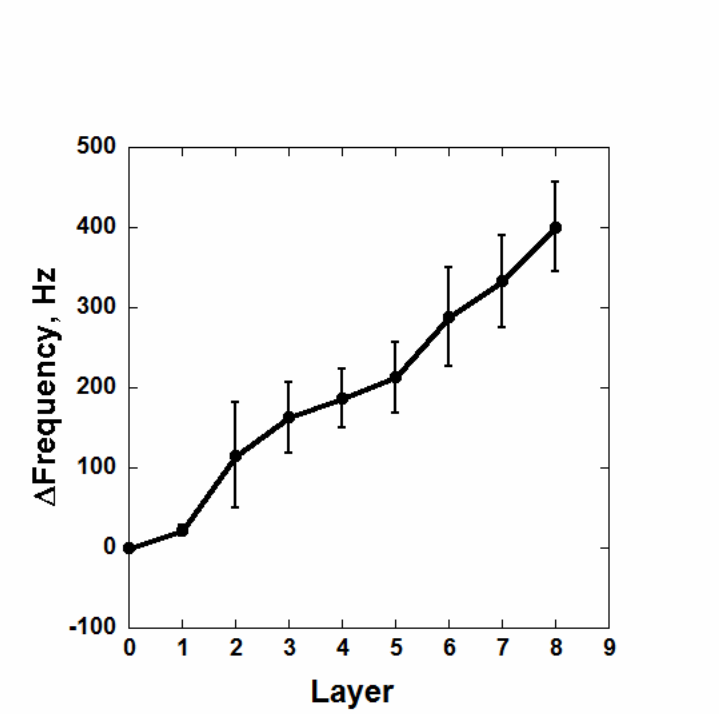

Figure S1. QCM frequency decreases indicating LBL film formation at the gold resonator. Initial frequency measured after MPA (3-mercaptopropionic acid) self assembly monolayer formation. PDDA (poly-(dially-dimethylammonium chloride), CAM (CYP101, Cytochrome P450cam).

Using equation 2 the estimated nominal film thickness was 6.4 ± 0.97nm. The amounts of DNA and CYP101 as approximated with the Sauerbrey equation (1) are 1.8 ± 0.72 pmoles/cm^2 and 0.122 ±0.07 pmoles/cm^2, respectively. These concentrations estimates the amounts present in the electrochemical experiments conducted.

Square Wave Voltammerty. PG electrodes with LBL films of DNA and CYP101 were incubated with styrene, hydrogen peroxide and various inhibitor concentrations followed by square wave voltammograms at each incubation times. Representative voltammograms for imidazole, imidazole-4-acetic acid and sulconazole at each inhibitor concentration are shown in Figures S2, S3, and S4, respectively. The voltammograms in the presence of inhibitor all increase incubation time (up to 1 min for imidazole and imidazole-4-acetic, 45 seconds for sulconazole). These voltammograms were used to generate sensor ratios of damage signals versus undamaged signals to determine the extent o DNA damage inhibition. By converting the voltammetric signals, the inhibitory effects can be readily compared to each other and to the uninhibited experiment.

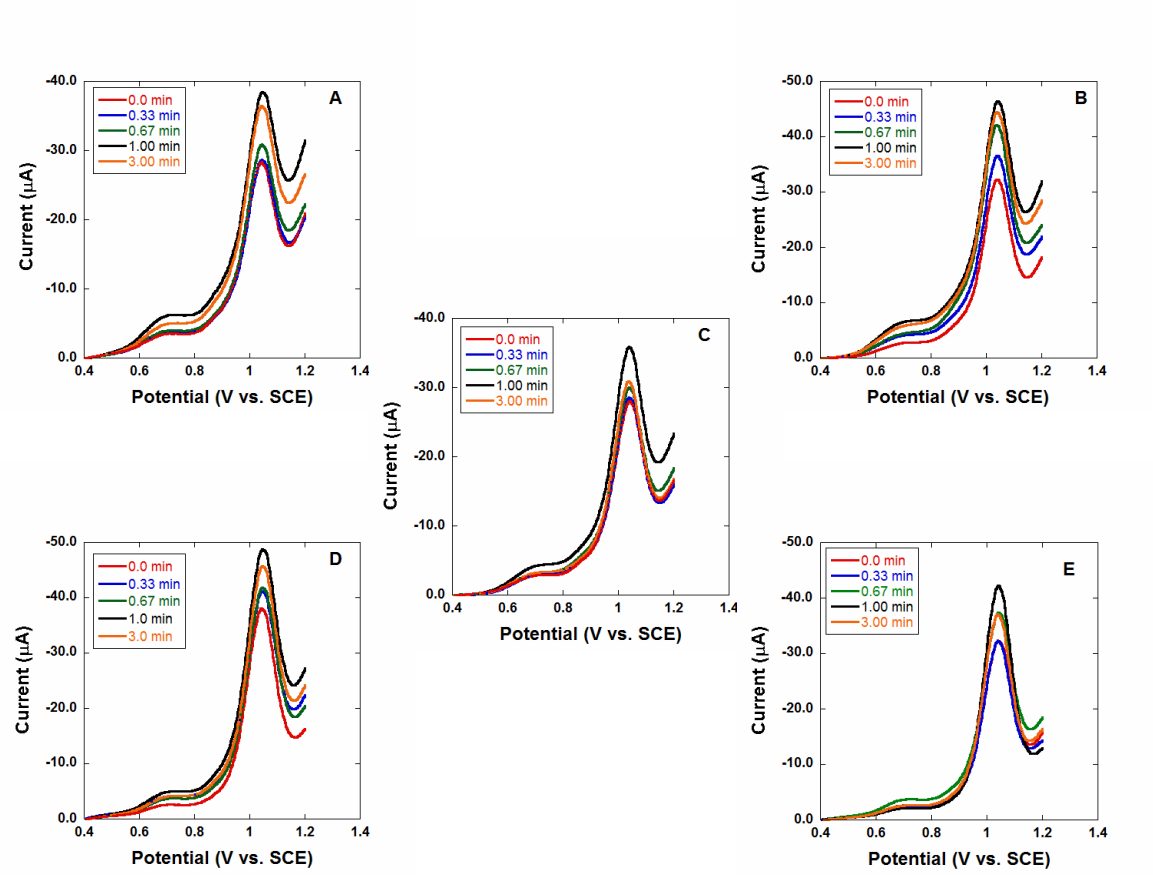

Figure S2. Square wave voltammetry (SWV) of (PDDA/DNA/CYP101/)$_2$ - PDDA/DNA films in 50 mM NaH_2PO_4 pH 7.0/50mM NaCl with 50µM $Ru(bpy)_3Cl_2$ as the mediator obtained with at various concentrations of imidazole. Incubations were conducted in 10mM sodium acetate pH 5.5/50mM NaCl at 37ºC with 2% styrene, 1mM H_2O_2 and a specific imidazole concentration. A) 50 µM, B) 100 µM, C) 150 µM, D) 250 µM, and E) 500 µM.

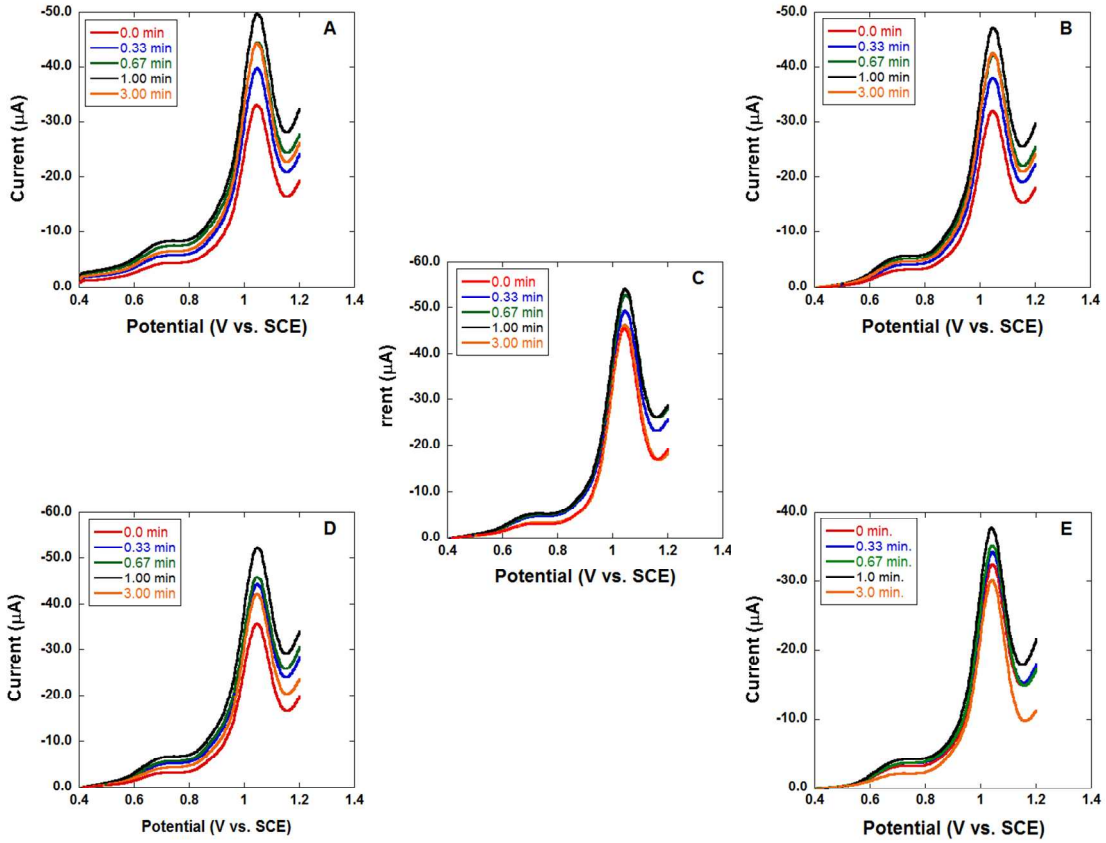

Figure S3. Square wave voltammetry (SWV) of (PDDA/DNA/CYP101/)$_2$ - PDDA/DNA films in 50 mM NaH_2PO_4 pH 7.0/50mM NaCl with 50µM $Ru(bpy)_3Cl_2$ as the mediator obtained with at various concentrations of imidazole-4-acetic acid. Incubations were conducted in 10mM sodium acetate pH 5.5/50mM NaCl at 37ºC with 2% styrene, 1mM H_2O_2 and a specific imidazole-4-acetic acid concentration. A) 50 µM, B) 100 µM, C) 150 µM, D) 250 µM, and E) 500 µM.

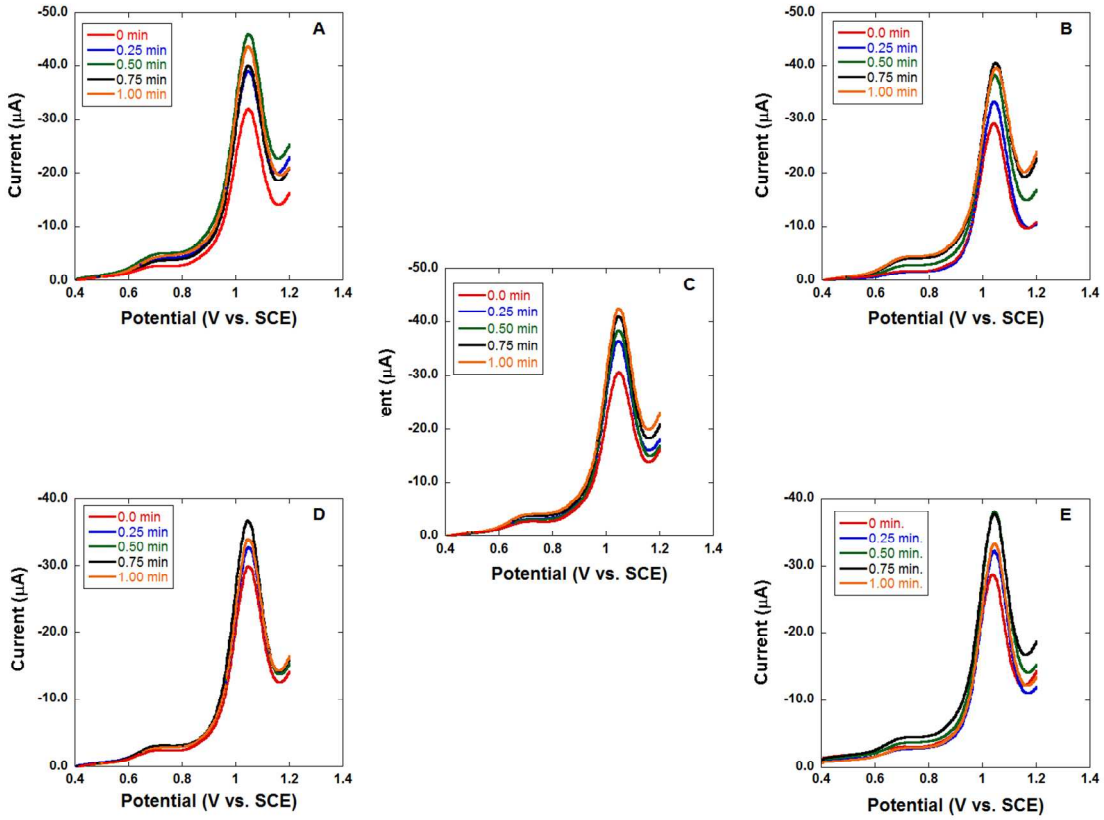

Figure S4. Square wave voltammetry (SWV) of (PDDA/DNA/CYP101/)$_2$ - PDDA/DNA films in 50 mM NaH_2PO_4 pH 7.0/50mM NaCl with 50µM $Ru(bpy)_3Cl_2$ as the mediator obtained with at various concentrations of sulconazole. Incubations were conducted in 10mM sodium acetate pH 5.5/50mM NaCl at 37ºC with 2% styrene, 1mM H_2O_2 and a specific sulconazole concentration. A) 50 µM, B) 100 µM, C) 150 µM, D) 250 µM, and E) 500 µM.

4-Methyl-2-phenylimidazole control. 4-methyl-2-phenylimidazole was used as negative control based on the disruption of N3 binding with 2 and 4 position substitution on the imidazole ring. By incubating at 500µM (concentration that displayed most inhibition, sensor ratios were generated from SWV analysis. The sensor ratios comparing 500µM 4methylimidazole and the uninhibited system are shown in Figure S5. The signals are similar indication the absence of effective inhibition.

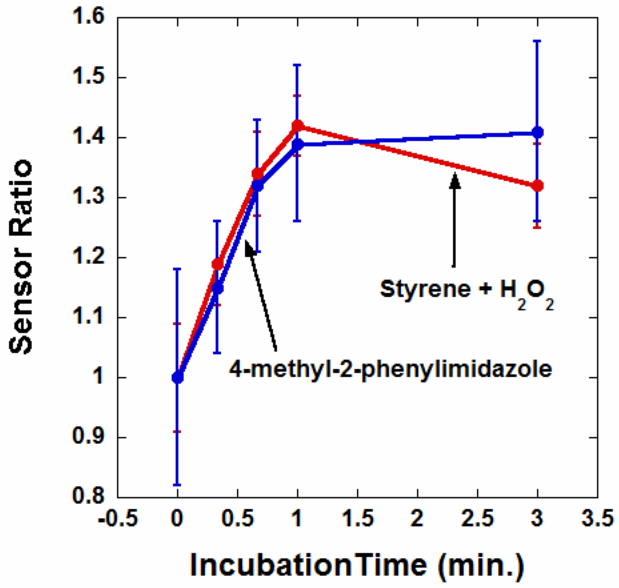

Figure S5. Sensor ratios generated from SWV analysis comparing 500µM 4methyl-2phenylimidazole and 2% styrene. Incubations were conducted in 10mM sodium acetate pH 5.5/50mM NaCl at 37ºC with 2% styrene, 1mM H_2O_2 and with and without 4methyl-2phenylimidazole.

Background Sensor Ratios. Sensor ratios were generated from SWV experiments with the inhibitors to demonstrate there minimal contribution to observed signals. 500µM concentrations of imidazole, imidazole-4-acetic acid and sulconazole were incubated in the absence of styrene and hydrogen peroxide to ensure no DNA damage signals arises. A comparison of sensor ratios for each inhibitor to the uninhibited signals is shown in Figure S6. Compared to the damage sensor ratios little signals were obtained with the inhibitors only.

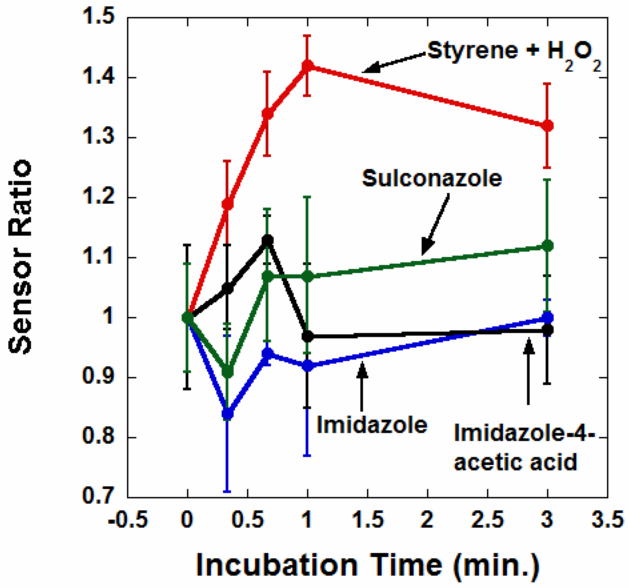

Figure S6. Background sensor ratios generated from SWV analysis of electrodes incubated with 500µM inhibitor only. Incubations were conducted in 10mM sodium acetate pH 5.5/50mM NaCl at 37ºC with 500µM of imidazole, imidazole-4-acetic acid and sulconazole. 50 mM NaH_2PO_4 pH 7.0/50mM NaCl with 50µM $Ru(bpy)_3Cl_2$ were used for electrochemical analyses.

Michaelis-Menten Inhibition Model Fits. Additional linear and nonlinear fits of inhibition trends using Michaelis-Menten inhibition models (eqs. 3, 4, 6 and 7) for imidazole (Figure S7), imidazole-4-acetic(Figure S7), and sulconazole (Figure S9). Each figure contain fits for competitive ($1/K_m$) (A), simple competitive with estimated values (B), Dixon linear competitive (C) and Dixon linear uncompetitive (D) models. Corresponding values of the apparent inhibition constant for each model is shown in Table 1. As described in the paper, these models yielded inadequate fits to the experimental trends, which were verified by the goodness of fit analysis.

Table S1 Values of inhibition constants as obtained from linear and nonlinear fits using the various inhibition mechanisms.

		Imidazole		Imidazole-4-acetic acid		Sulconazole	
Model	P[c]	Value	R^2	Value	R^2	Value	R^2
Comp. K_m^{-1}	K_I^{*} [a]	4.0 ± 0.9	0.44	2.2 ± 0.5	0.67	1.8 ± 0.5	0.64
Uncomp.	$K_I^{*'}$	268.2 ± 59.8	0.44	149.8 ± 31.42	0.67	124.0 ± 30.1	0.64
Simple Comp. (val.)	K_I^{*}	89.5 ±66.3	0.61	67.3 ± 42.1	0.75	58.1 ± 44.7	0.68
	V_1 [b]	0.06 ± 0.03		0.04 ± 0.02		0.04 ± 0.03	
Simple Comp.	K_I^{*}	245.0 ± 139.3	0.96	142.3 ± 4.5	0.98	204.2 ± 154.2	0.92
	V_m [b]	0.15 ± 0.01		0.14 ± 0.01		0.14 ± 0.01	
	V_1	0.05 ± 0.02		0.03 ± 0.01		0.01 ± 0.04	
DLC	K_I^{*}	5.3 ± 0.8	0.58	3.2 ± 0.37	0.76	2.1 ± 0.2	0.91
DLU	$K_I^{*'}$	360.0 ± 51.6	0.58	213.3 ± 25.1	0.76	139.0 ± 12.5	0.91

All cases except the simple competitive mechanism (no estimated values) employed both the apparent K_m^{*} and V_m^{*}. [a] In units of micromolar. [b] V_m, V_1 (in units of min^{-1}). [c] Unknown parameter evaluated by fitting. V_1 in the simple competitive mechanisms is the maximal velocity associated with enzyme-inhibitor complex.[2] Abbreviations: Comp. (Competitive, eq. 3), Uncomp. (Uncompetitive, eq. 4), DLC (Dixon linear competitive, linearized eq. 3), DLU (Dixon linear Uncompetitive, linearized eq. 4), Comp. Km^{-1} (rearranged competitive model caused by division of K_m, eq. 7), Simple Comp. (Simple competitive model eq. 6).

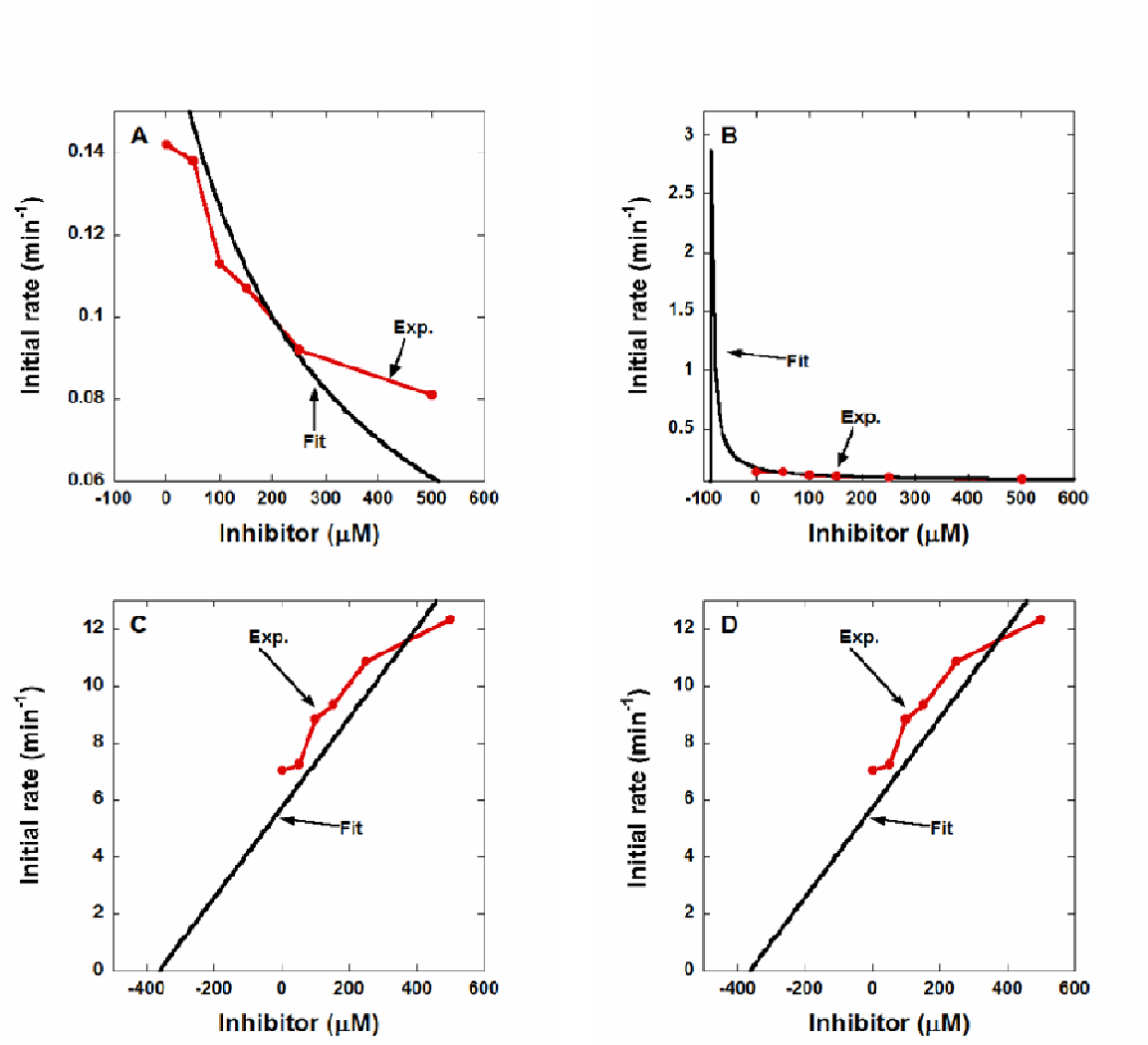

Figure S7. Nonlinear and linear fits of the imidazole inhibition trend towards the evaluation of the apparent K_I^*. A) Competitive (1/Km) (eq. 7), B) Simple competitive (with estimated value of V_m^*) (eq. 6) C) Dixon Linear Competitive (eq. 3), and D) Dixon Linear Uncompetitive (eq. 4). The apparent K_m and V_m values were used these fits. An estimated K_I value of 100μM was used as starting point for iteration.

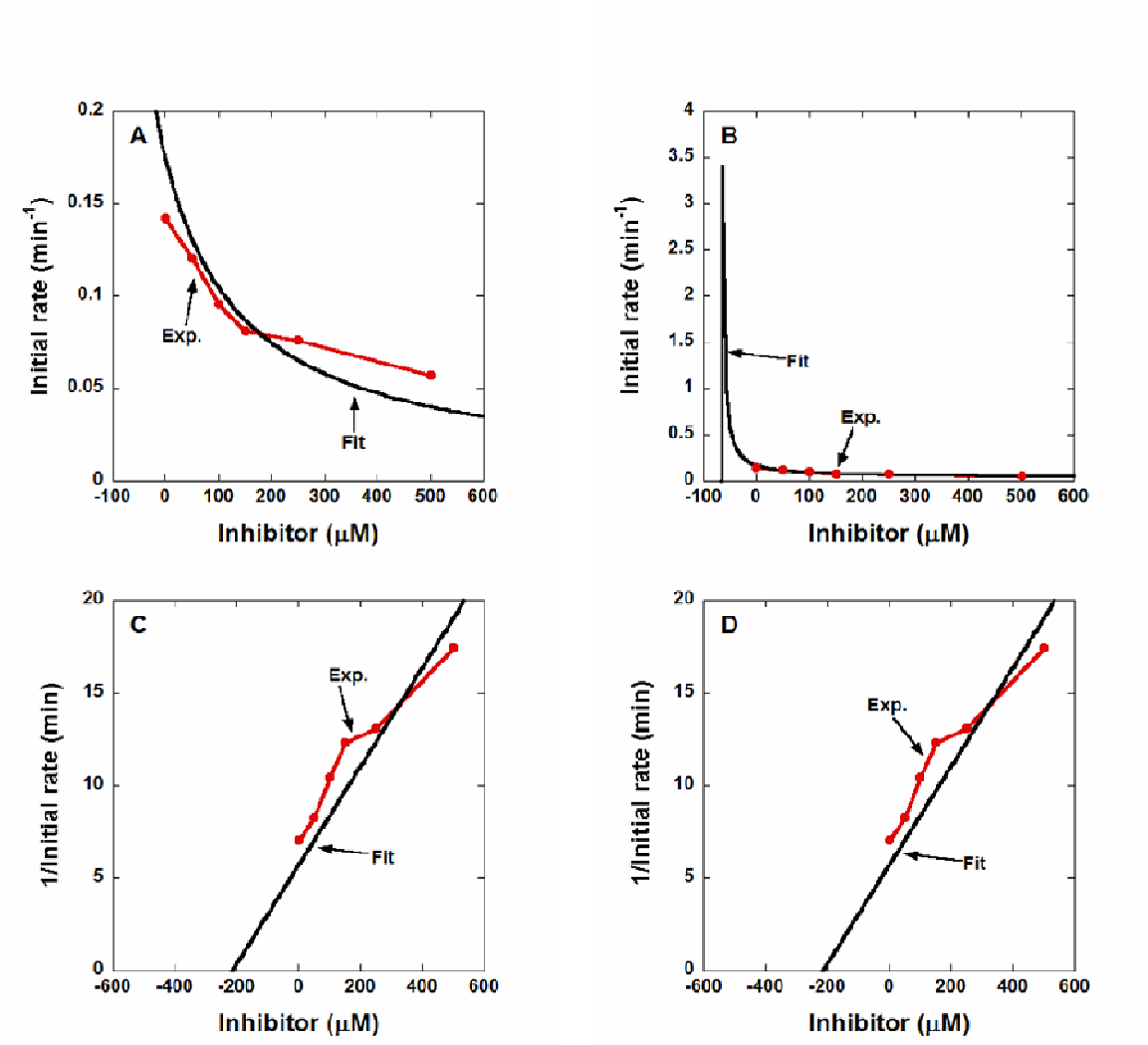

Figure S8. Nonlinear and linear fits of the imidazole-4-acetic acid inhibition trend towards the evaluation of the apparent K_I^*. A) Competitive (1/Km) (eq. 7), B) Simple competitive (with estimated value of V_m^*) (eq. 6) C) Dixon Linear Competitive (eq. 3), and D) Dixon Linear Uncompetitive (eq. 4). The apparent K_m and V_m values were used these fits. An estimated K_I value of 100μM was used as starting point for iteration.

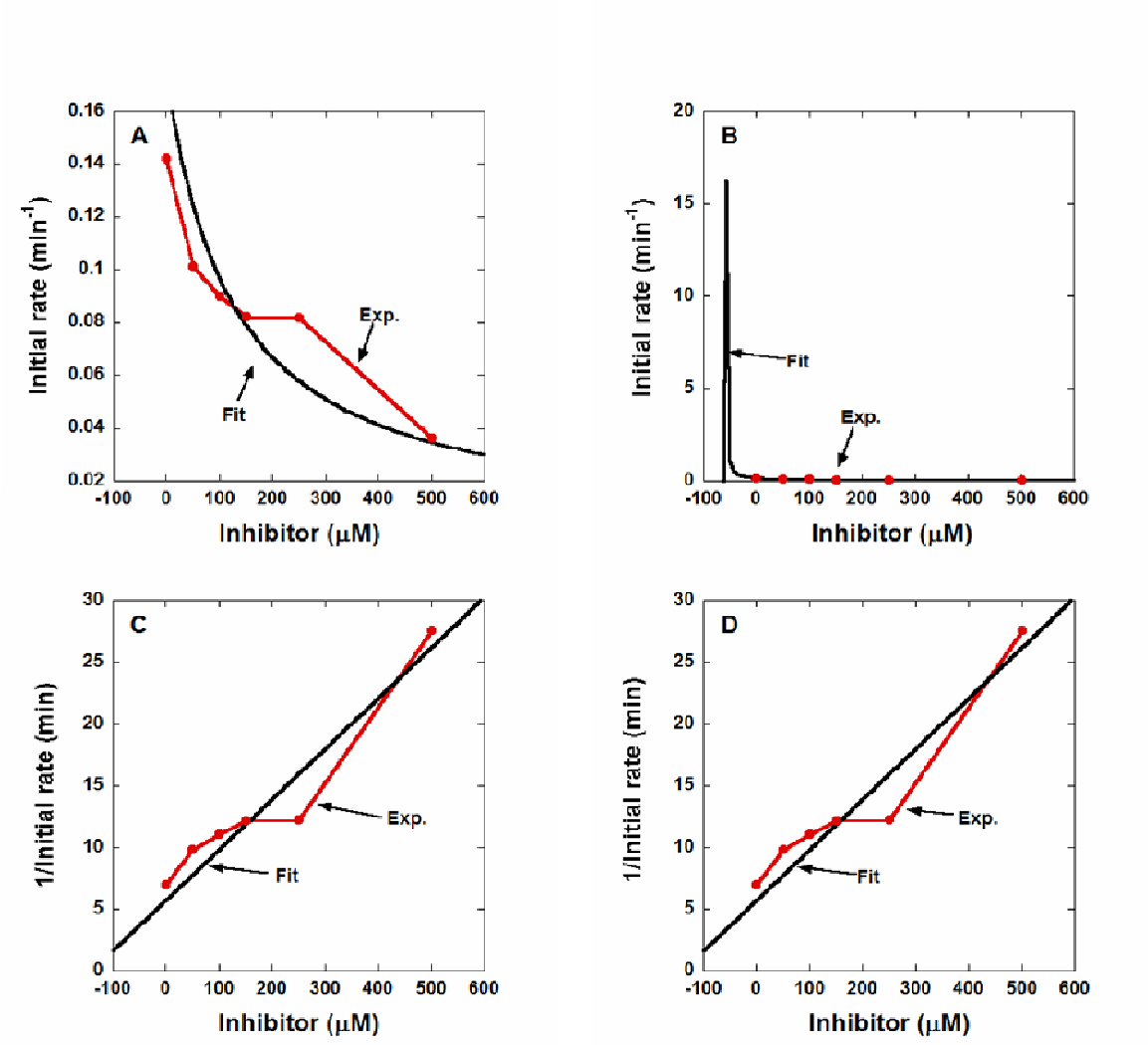

Figure S9. Nonlinear and linear fits of the sulconazole inhibition trend towards the evaluation of the apparent K_I^*. A) Competitive (1/Km) (eq. 7), B) Simple competitive (with estimated value of V_m^*) (eq. 6) C) Dixon Linear Competitive (eq. 3), and D) Dixon Linear Uncompetitive (eq. 4). The apparent K_m and V_m values were used these fit. An estimated K_I value of 100μM was used as starting point for iteration.

References

(1) Lvov, Y. M.; Lu, Z.; Schenkman, J. B.; Zu, X.; Rusling, J. F. *J. Am. Chem. Soc.* **1998**, *120*, 4073-4080.

(2) Rusling, J. F.; Kumosinski, T. In *Nonlinear Computer Modeling of Chemical and Biochemical Data*; Academic Press: 1996.